Mesophase Structures of Higher Alkanoyl Derivatives of 6,6′-Diamino-2,2′-bipyridine and Their Metal Complexes

Takashi KUBOKI, Koji ARAKI, Masaki YAMADA, and Shinsaku SHIRAISHI*
Institute of Industrial Science, The University of Tokyo, 7-22-1 Roppongi, Minato-ku, Tokyo 106
(Received October 5, 1993)

New Cu(II), Ni(II), Co(II), and Pd(II) complexes of higher alkanoyl derivatives of 6,6′-diamino-2,2′-bipyridine were synthesized and their mesogenic properties were investigated. The Cu(II) complexes appear to exhibit a smectic C structure in their mesophase state.

Recently, thermotropic liquid crystals of transition metal complexes have been studied for their characteristic electrical, magnetic, and optical properties. Most of these complexes have two to eight alkyl chains and a tetradentate square planer core with a tetradentate ligand, porphyrin[1,2] or phthalocyanine[3,4] or such a didentate ligand as β-diketone.[5]

We have reported 6,6′-diamino-2,2′-bipyridine derivatives as new ligands of the N_2O_2 type square planar complexes, and described their thermal and chemical stabilities.[6,7] In this paper, we report divalent transition metal complexes of 6,6′-bis(alkanoylamino)-2,2′-bipyridine and 2-(alkanoylamino)pyridine, and the effects of the central metal and the length of alkyl chains on their thermal properties.

Experimental

Measurements. ^{1}H and ^{13}C NMR spectra were recorded on JEOL FX-100 or GX-270 spectrometer in $CDCl_3$ using TMS as an internal standard. IR spectra were measured with a JASCO IR-700 spectrophotometer. Magnetic properties were determined with a Shimadzu MB-11 magnetic balance. Differential scanning calorimetry (DSC) was performed on Perkin–Elmer DSC-2 under a nitrogen atmosphere. Powder X-ray diffraction patterns were measured with Cu-$K\alpha$ radiation, using a Rigaku RU-200 with a homemade heating stage and a thermoregulator.

Materials. 6,6′-Bis(lauroylamino)-2,2′-bipyridine (H_2LC_{12}): To a pyridine solution (10 cm^3) of 6,6′-diamino-2,2′-bipyridine (0.19 g, 1 mmol) on an ice bath, lauroyl chloride (2.4 ml, 10 mmol) in pyridine (10 cm^3) was added, and the mixture was allowed to react for 30 min. The reaction mixture was then poured into methanol (100 cm^3), and the precipitate was collected, and washed successively with a dilute HCl solution, a dilute ammonia solution, water, and methanol. Recrystallization from benzene gave colorless plates (0.36 g, 65%): Mp 440 K. Found: C, 73.93; H, 10.31; 10.27%. Calcd for $C_{34}H_{54}N_4O_2$: C, 74.14; H, 9.88; N, 10.17%. IR (KBr) 3258 (NH), 2916, 2850 (CH_2), 1668 (amide I), 1537 (amide II), and 1258 (amide III) cm^{-1}; ^{1}H NMR ($CDCl_3$) δ=0.89 (6H, t, CH_3), 1.29—1.52 (32H, m, CH_2), 1.77 (4H, m, CH_2), 2.44 (4H, t, CH_2), 7.19 (2H, s, NH), 7.72—8.01 (4H, m), 8.25 (2H, d).

6,6′-Bis(mirystoylamino)-2,2′-bipyridine (H_2LC_{14}): Yield 64%: Mp 433 K. Found: C, 75.20; H, 10.36; N, 8.82%. Calcd for $C_{38}H_{62}N_4O_2$: C, 75.20; H, 10.30; N, 9.23%. IR (KBr) 3266 (NH), 2916, 2850 (CH_2), 1670 (amide I), 1538 (amide II), and 1259 (amide III) cm^{-1}; ^{1}H NMR ($CDCl_3$) δ=0.90 (6H, t, CH_3), 1.28—1.52 (40H, m, CH_2), 1.76 (4H, m, CH_2), 2.44 (4H, t, CH_2), 7.19 (2H, s, NH), 7.73—8.01 (4H, m), 8.24 (2H, d).

6,6′-Bis(palmitoylamino)-2,2′-bipyridine (H_2LC_{16}): Yield 82%: Mp 428 K. Found: C, 76.33; H, 10.92; N, 8.12%. Calcd for $C_{42}H_{70}N_4O_2$: C, 76.08; H, 10.64; N, 8.45%. IR (KBr) 3264 (NH), 2914, 2848 (CH_2), 1669 (amide I), 1531 (amide II), and 1259 (amide III) cm^{-1}; ^{1}H NMR ($CDCl_3$) δ=0.90 (6H, t, CH_3), 1.28—1.52 (48H, m, CH_2), 1.77 (4H, m, CH_2), 2.44 (4H, t, CH_2), 7.19 (2H, s, NH), 7.72—8.01 (4H, m), 8.24 (2H, d).

6,6′-Bis(stearoylamino)-2,2′-bipyridine (H_2LC_{18}): Yield 61%: Mp 421 K. Found: C, 77.03; H, 10.96; N, 7.77%. Calcd for $C_{46}H_{78}N_4O_2$: C, 76.83; H, 10.93; N, 7.79%. IR (KBr) 3266 (NH), 2914, 2848 (CH_2), 1670 (amide I), 1538 (amide II), and 1259 (amide III) cm^{-1}; ^{1}H NMR ($CDCl_3$) δ=0.90 (6H, t, CH_3), 1.28—1.52 (56H, m, CH_2), 1.77 (4H, m, CH_2), 2.44 (4H, t, CH_2), 7.19 (2H, s, NH), 7.72—8.01 (4H, m), 8.24 (2H, d).

6,6′-Bis(arachidoylamino)-2,2′-bipyridine (H_2LC_{20}): Yield 29%: Mp 421 K. Found: C, 77.58; H, 11.75; N, 6.88%. Calcd for $C_{50}H_{86}N_4O_2$: C, 77.46; H, 11.18; N, 7.23%. IR (KBr) 3316 (NH), 2918, 2850 (CH_2), 1674 (amide I), 1531 (amide II), and 1258 (amide III) cm^{-1}; ^{1}H NMR ($CDCl_3$) δ=0.90 (6H, t, CH_3), 1.29—1.49 (64H, m, CH_2), 1.78 (4H, m, CH_2), 2.45 (4H, t, CH_2), 7.20 (2H, s, NH), 7.72—8.01 (4H, m), 8.24 (2H, d).

2-(Palmitoylamino)pyridine ($HL'C_{16}$): To a methylene chloride solution (15 cm^3) of 2-aminopyridine (0.96 g, 10 mmol) and triethylamine (1.21 g, 12 mmol) on an ice bath, palmitoyl chloride (2.76 g, 10 mmol) in methylene chloride (15 cm^3) was added, and the mixture was allowed to react for 30 min. The reaction mixture was then filtered and evaporated to collect the crude product. Recrystallizations from a methanol solution of KOH and then from methanol gave colorless plates (2.70 g, 81%): Mp 342 K. Found: C, 75.03; H, 11.47; N, 8.24%. Calcd for $C_{21}H_{36}N_2O$: C, 74.59; H, 11.59; N, 8.04%. IR (KBr) 3352 (NH), 2916, 2850 (CH_2), 1687 (amide I), 1533 (amide II), and 1242 (amide III) cm^{-1}; ^{1}H NMR ($CDCl_3$) δ=0.88 (3H, t, CH_3), 1.25—1.31 (24H, m, CH_2), 1.70 (2H, m, CH_2), 2.38 (2H, t, CH_2), 7.02 (1H, dd), 7.70 (1H, dd), 8.23 (1H, d) 8.26 (1H, d), 8.41 (1H, s, NH).

Cu(LC_{12}): H_2LC_{12} (0.28 g, 0.50 mmol) and [Cu(NO_3)$_2$](H_2O)$_3$ (0.12 g, 0.5 mmol) were dissolved in methanol (200 cm^3) and were allowed to react for 2 h. A 1/2 M KOH ethanol solution (4 cm^3, 1 M=1 mol dm^{-3}) was added and the mixture was stirred for another 1 h. The precipitate was collected and then washed with methanol.

Recrystallization from benzene gave brown needles. Yield 72%. Found: C, 66.34; H, 8.49; N, 8.96%. Calcd for $C_{34}H_{52}N_4O_2Cu$: C, 66.69; H, 8.56; N, 9.15%. IR (KBr) 2918, 2848 (CH_2), 1556 (amide I), 1388 (amide II) cm^{-1}.

Cu(LC_{14}): Yield 76%. Brown needles. Found: C, 67.31; H, 8.53; N, 9.57%. Calcd for $C_{38}H_{60}N_4O_2Cu$: C, 68.28; H, 9.05; N, 8.38%. IR (KBr) 2918, 2848 (CH_2), 1557 (amide I), and 1387 (amide II) cm^{-1}.

Cu(LC_{16}): Yield 90%. Brown needles. Found: C, 69.60; H, 10.14; N, 7.59%. Calcd for $C_{42}H_{68}N_4O_2Cu$: C, 69.62; H, 9.46; N, 7.73%. IR (KBr) 2916, 2848 (CH_2), 1556 (amide I), and 1389 (amide II) cm^{-1}.

Cu(LC_{18}): Ethanol was used for solvent: Yield 73%; Brown powder. Found: C, 70.85; H, 10.07; N, 7.34%. Calcd for $C_{46}H_{76}N_4O_2Cu$: C, 70.77; H, 9.81; N, 7.18%. IR (KBr) 2916, 2848 (CH_2), 1557 (amide I), 1387 (amide II) cm^{-1}.

Cu(LC_{20}): Ethanol was used for solvent: Yield 75%; Brown powder. Found: C, 72.21; H, 10.43; N, 7.49%. Calcd for $C_{50}H_{84}N_4O_2Cu$: C, 71.77; H, 10.12; N, 6.70%. IR (KBr) 2916, 2848 (CH_2), 1557 (amide I), and 1391 (amide II) cm^{-1}.

Ni(LC_{16}): H_2LC_{16} (0.28 g, 0.50 mmol) and $[Ni(NO_3)_2](H_2O)_6$ (0.15 g, 0.50 mmol) were dissolved in methanol (200 cm^3) and the mixture was allowed to react for 2 h. A 1/2 M KOH ethanol solution (4 cm^3) was added and the mixture was stirred for another 1 h. The precipitate was collected and then washed with methanol. Recrystallization from benzene gave yellow needles. 0.26 g, Yield 73%. Found: C, 69.63; H, 9.83; N, 7.93%. Calcd for $C_{42}H_{68}N_4O_2Ni$: C, 70.09; H, 9.52; N, 7.78%. IR (KBr) 2916, 2850 (CH_2), 1558 (amide I), and 1399 (amide II) cm^{-1}; ^1H NMR ($CDCl_3$) δ=0.87 (6H, t, CH_3), 1.25 (48H, m, CH_2), 1.63 (4H, m, CH_2), 2.44 (4H, t, CH_2), 7.05 (2H, d), 7.33 (2H, d), 7.73 (2H, dd); ^{13}C NMR ($CDCl_3$) δ=14.1, 22.7, 27.1, 29.4, 29.5, 29.7, 31.9, 39.1, 112.9, 123.5, 138.4, 151.7, 155.6, 176.7.

Co(LC_{16}): H_2LC_{16} (0.28 g, 0.50 mmol) and $[Co(OAc)_2](H_2O)_4$ (0.31 g, 0.50 mmol) were dissolved in ethanol (200 cm^3) under a nitrogen atmosphere on a water bath thermostated at 40 °C, and the mixture was allowed to react for 1 h. A 1/2 M KOH ethanol solution (4 cm^3) was added and the mixture was stirred for another 1 h. The precipitate was collected and then washed with methanol. Recrystallization from benzene gave red powder. 0.27 g, Yield 75%; Found: C, 70.19; H, 10.33; N, 7.98%. Calcd for $C_{42}H_{68}N_4O_2Co$: C, 70.07; H, 9.52; N, 7.78%. IR (KBr) 2918, 2850 (CH_2), 1554 (amide I), and 1389 (amide II) cm^{-1}.

Pd(LC_{16}): To a suspension of $PdCl_2$ (0.12 g, 0.65 mmol) in ethanol (100 cm^3), LiCl was added until $PdCl_2$ was dissolved. H_2LC_{16} (0.28 g, 0.50 mmol) was then added and the mixture was stirred until dissolved and allowed to react for another 1 h. A 1/2 M KOH ethanol solution (4 cm^3) was added and the mixture was stirred for another 1 h. The precipitate was collected and then washed with methanol. Recrystallization from benzene gave yellow powder. Yield 10%. Found: C, 65.57; H, 9.49; N, 7.24%. Calcd for $C_{42}H_{68}N_4O_2Pd$: C, 65.73; H, 8.93; N, 7.30%. IR (KBr) 2916, 2848 (CH_2), 1562 (amide I), and 1382 (amide II) cm^{-1}; ^1H NMR ($CDCl_3$) δ=0.87 (6H, t, CH_3), 1.25 (48H, s, CH_2), 1.80 (4H, m, CH_2), 2.58 (4H, t, CH_2), 7.18 (2H, d), 7.44 (2H, d), and 7.79 (2H, dd); ^{13}C NMR ($CDCl_3$) δ=14.8, 23.4, 28.5, 30.1, 30.4, 32.7, 40.5, 114.6, 125.4, 139.0, 153.1, 154.0, and 175.6.

Pd($L'C_{16}$)$_2$: In a manner similar to that for Pd(LC_{16}), $[Pd(L'C_{16})_2](H_2O)_2$ was collected (Found C, 62.38; H, 9.09; N, 6.96%. Calcd for $[Pd(L'C_{16})_2](H_2O)_2$: C, 62.63; H, 9.26; N, 6.96%). The color of the product turned black at the melting point without weight loss. After heating at a temperature above the melting point, the sample showed ν_{N-H} at 3350 cm^{-1} and $\nu_{C=O}$ at 1687 cm^{-1} in the IR spectrum, to suggest that the complex turned into $HL'C_{16}$ and Pd(OH)$_2$ (Scheme 1). The coordinated H_2O molecules were removed by treatment with pyridine. $[Pd(L'C_{16})_2](H_2O)_2$ was dissolved in a 5% pyridine solution in methylene chloride and the mixture was stirred for 1 h. The solution was evaporated, heated in vacuum, then recrystallized from benzene. Yield 10%; Yellow powder. Found: C, 65.58; H, 9.43; N, 7.37%. Calcd for $C_{42}H_{70}N_4O_2Pd$: C, 65.56; H, 9.17; N, 7.28%. IR (KBr) 2912, 2848 (CH_2), 1568 (amide I), and 1383 (amide II) cm^{-1}; ^1H NMR ($CDCl_3$) δ=0.87 (6H, t, CH_3), 1.24 (48H, s, CH_2), 1.71 (4H, m, CH_2), 2.47 (4H, t, CH_2), 6.91 (2H, dd), 7.13 (2H, d), 7.66 (2H, dd), and 8.51 (2H, d); ^{13}C NMR ($CDCl_3$) δ=14.8, 23.4, 27.9, 30.1, 30.4, 32.7, 39.8, 117.4, 123.7, 139.7, 144.5, 154.3, and 173.6.

Results and Discussion

Synthesis. Ligands H_2LC_n (n=12—20) and $HL'C_{16}$ were synthesized from 6,6′-diamino-2,2′-bipyridine and 2-aminopyridine, and the corresponding acid chloride. Cu(II), Ni(II), Co(II), and Pd(II) complexes of H_2LC_n, M(LC_n), were synthesized using $Cu(NO_3)_2$, $Ni(NO_3)_2$, $Co(OAc)_2$, and $Li_2[PdCl_4]$ in methanol or ethanol, respectively. $HL'C_{16}$ formed a deprotonated complex with Pd(II), and an M(OH)$_2$ was collected by addition of KOH to the solution of the protonated complexes of Cu(II), Ni(II), and Co(II).

Thermal Properties of Complexes. The thermal properties of the complexes were studied with DSC. Pd(II) complexes, Pd(LC_{16}) and Pd($L'C_{16}$)$_2$, showed an endothermic peak at T_m, 391 and 396 K, respectively, during heating, and did not show any mesophase transition. As-prepared Ni(LC_{16}) and Co(LC_{16}) also showed only an endothermic peak at T_m, 376 and 386 K, respectively, in the first heating process. Heat-treated Ni(LC_{16}) showed two unresolved endothermic peaks at 336 and 366 K in addition to T_m at 352 K and T_c at 379 K in the heating stage. Similarly, heat-treated Co(LC_{16}) showed two endothermic peaks at 336 and 352 K in addition to T_m at 366 K and T_c at 379 K in the heating stage. The additionally appearing endothermic peaks observed in heat-treated Ni(LC_{16}) and Co(LC_{16}) may be due to a mesophase transition, but further studies were not carried out because of their narrow temperature range.

While as-prepared Cu(II) complexes, Cu(LC_n), showed a broad endothermic peak at T_m besides a clearing point in the first heating process (Table 1), heat-treated Cu(LC_n) showed sharp endothermic peaks at T_m, and Cu(LC_{18}) and Cu(LC_{20}) showed two endothermic peaks and one exothermic peak besides T_m (Fig. 1). The broad endothermic peaks of as-prepared complexes suggest the existence of a disorder in the crystal struc-

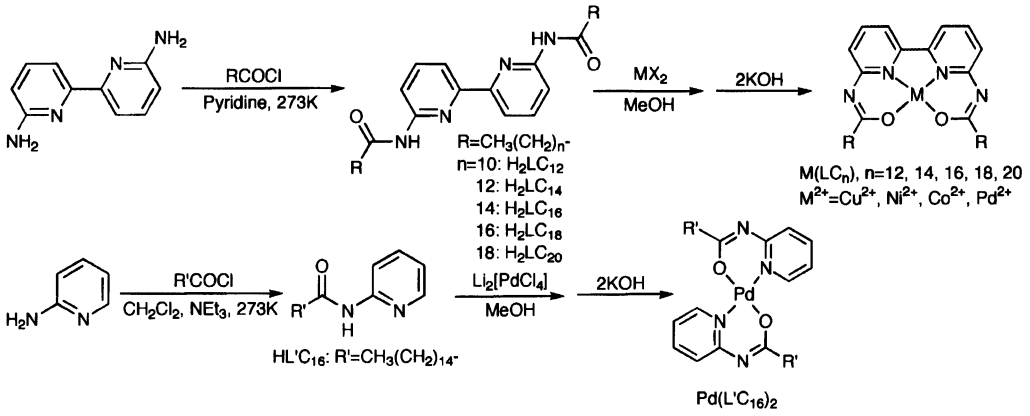

Scheme 1.

Table 1. T_m and T_c/K of As-Prepared Cu(II) Complexes in the First Heating Process

Complexes	T_m	T_c
$Cu(LC_{12})$	353	405
$Cu(LC_{14})$	361	403
$Cu(LC_{16})$	367	401
$Cu(LC_{18})$	370	397
$Cu(LC_{20})$	375	395

Heating rate: 5 K min^{-1}.

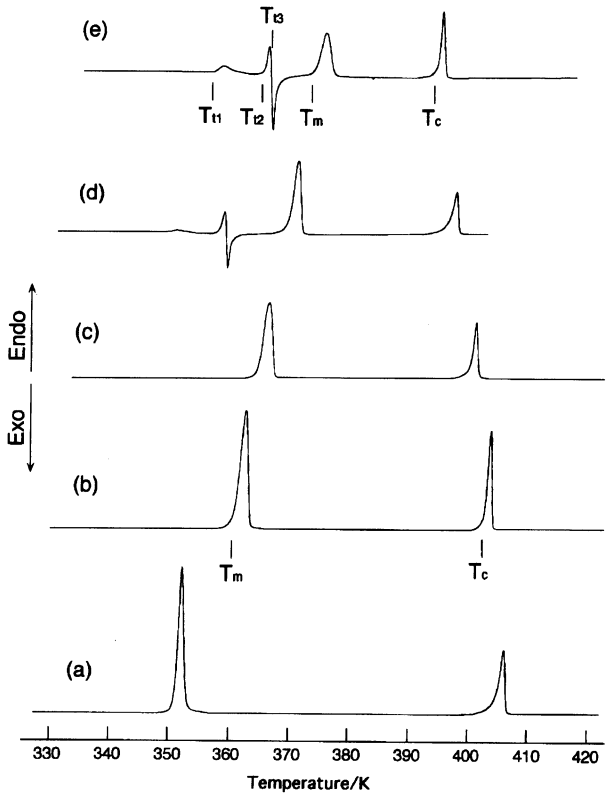

Fig. 1. DSC curves for $Cu(LC_n)$. Heating rate: 5 K min^{-1}. (a): $n=12$; (b): $n=14$; (c): $n=16$; (d): $n=18$; (e): $n=20$.

ture of as-prepared samples. The complexes are softened at a temperature between T_m and T_c. The ΔH_c values are almost constant, and ΔH_m increases with the carbon number for $n \leqq 16$. It is hence suggested that T_m and T_c are the melting point of alkyl groups and that of the plane core groups, respectively. The complicated thermograms of $Cu(LC_{18})$ and $Cu(LC_{20})$ at a heating rate of 5 K min^{-1} became simplified by a slower heating rate, 1.25 K min^{-1} (Fig. 2). The endo- and exothermic peaks at T_{t1}, T_{t2}, and T_{t3} almost disappeared and ΔH_m increased whereas the ΔH_c values remained constant (Table 2, Fig. 2), to show that ΔH_m of all the Cu(II) complexes, $Cu(LC_n)$, increases with the carbon number. This observation suggests that the characteristic endo- and exothermic peaks of $Cu(LC_{18})$ and $Cu(LC_{20})$ observed at a faster heating rate, 5 K min^{-1}, are due to rearrangement or restacking of the alkyl groups.

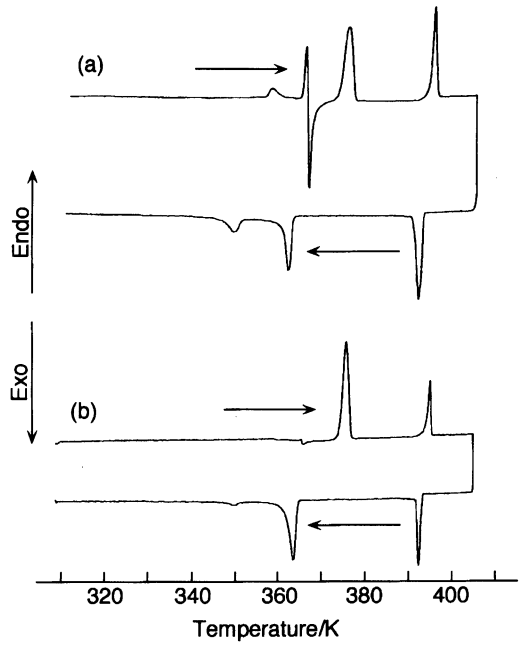

Fig. 2. DSC curves for $Cu(LC_{20})$. Heating rate; (a): 5 K min^{-1}; (b) 1.25 K min^{-1}.

Table 2. T_t, T_m, and T_c/K and ΔH/kJ mol^{-1} of Heat-Treated Cu(II) Complexes in Heating Process

Complexes	T_{t1}	ΔH_{t1}	T_{t2}	ΔH_{t2}	T_{t3}	ΔH_{t3}	T_m	ΔH_m	T_c	ΔH_c
$Cu(LC_{12})$[a]	—	—	—	—	—	—	351	58.6	405	32.6
$Cu(LC_{14})$[a]	—	—	—	—	—	—	361	64.0	403	31.8
$Cu(LC_{16})$[a]	—	—	—	—	—	—	365	70.3	401	32.2
$Cu(LC_{18})$[a]	349	3.8	358	8.4	359	21.8[c]	370	64.4	396	31.8
$Cu(LC_{18})$[b]	—	—	—	—	—	—	371	84.9	397	29.3
$Cu(LC_{20})$[a]	357	7.1	366	13.0	367	31.8[c]	374	53.1	394	33.5
$Cu(LC_{20})$[b]	—	—	—	—	—	—	375	101	395	33.1

a) Heating rate: 5 K min^{-1}. b) Heating rate: 1.25 K min^{-1}. c) Exothermic peak.

Fig. 3. Optical texture of $Cu(LC_{16})$ observed with crossed polarizers at 380 K.

Optical Texture of Complexes. Below T_c, Ni(LC_{16}) and Co(LC_{16}) showed a complicated optical texture under crossed polarizers, and Pd(LC_{16}) and Pd($L'C_{16}$)$_2$ did not show such a texture below T_m. It is

therefore suggested that the Pd(II) complexes are disordered in the solid state. Cu(LC_n) also showed a complicated texture for $n \geqq 14$. During cooling, the growth of layers parallel to the glases was observed, and the textures are not affected with endothermic peaks down to room temperature. This suggests that the structures of the solid phase are similar to those at the mesophase. The texture of Cu(LC_{16}) at 380 K, obtained by cooling the isotropic liquid phase, is shown in Fig. 3.

Magnetic Properties of Cu(II) Complex. The magnetic properties of heat-treated Cu(LC_{18}) in the solid state were measured at 77—400 K. The μ_{eff} values were 1.79±0.03 B.M. (B.M.=9.27×10^{-24} J T^{-1}), and a slight discontinuity of χ_{mol} is observed at a temperature near T_m (Fig. 4). This is suggestive of a slight change in the magnetic interaction, probably due to a difference in the distance of center metals between the solid phase and the mesophase.

X-Ray Diffraction of Cu(II) Complexes. The powder X-ray diffraction patterns of heat-treated Cu(II) complexes were measured at RT and 380 K. The patterns of Cu(LC_{16}) are shown in Fig. 5, and the principal lattice spacings of the Cu(II) complexes are given in Tables 3, 4, 5, 6, 7, 8, 9, 10, 11, and 12.

Cu(LC_{16}) at 380 K showed peaks at 16.1, 10.9, 8.19, 6.55, 4.68, and 4.09 Å, and the spacings are hence exactly in a ratio $1/2:1/3:1/4:1/5:1/7:1/8$. There are no spacings in a ratio $1:1/\sqrt{2}:1/\sqrt{3}$ in the narrow angle. This suggests that the complex forms a smectic phase, and the spacings are assigned to (002), (003), (004), (005), (007), and (008) planes, respectively (c= 32.8 Å). The CPK model of Cu(LC_{16}) indicates that the length of complexes is about 27.4 Å, to suggest that the complex forms a dimer in the layer. Cu(salen) is reported to form dimers in the crystalline state,[8] and the distance of two copper atoms is 3.22 Å. It is hence suggested that the spacing at 3.38 Å corresponds to the intra dimer spacing in the smectic phase (a=3.38 Å).

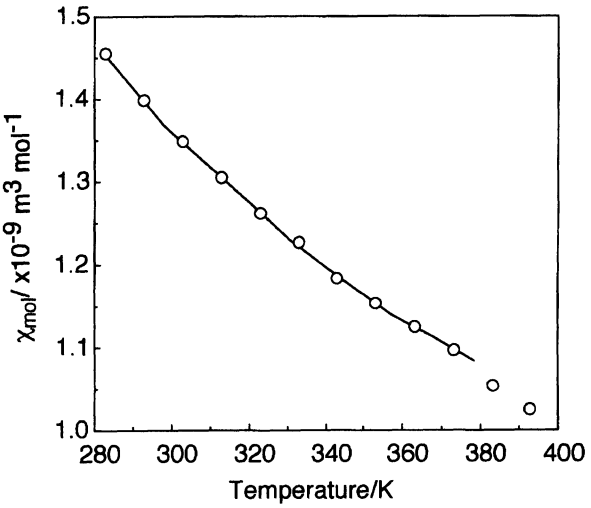

Fig. 4. Effect of temperature on χ_{mol} of Cu(LC_{18}).

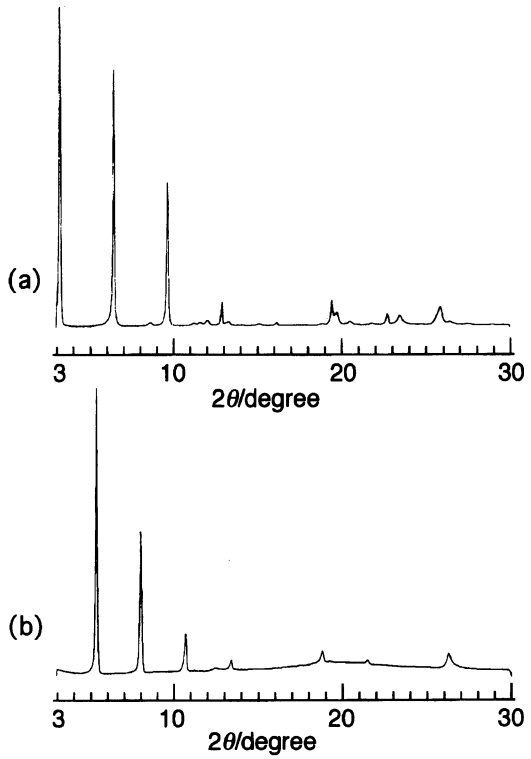

Fig. 5. X-Ray diffraction patterns of Cu(LC_{16}). Temperature; (a): RT; (b): 380 K.

Table 3. X-Ray Diffraction Data for Cu(LC_{12}) at RT

Measured lattice spacing /Å	Calculated lattice spacing /Å	(hkl)
22.2	22.2	(001)
11.1	11.1	(002)
9.02	9.02	(010)
7.42	7.42	(003)
5.56	5.56	(004)
4.66	—	—
4.44	4.45	(005)
4.01	—	—
3.70	3.71	(006)
3.44	3.45	(100)
3.25	3.22	(110)

a=3.45 Å, b=9.02 Å, c=22.2 Å.

Table 4. X-Ray Diffraction Data for Cu(LC_{12}) at 380 K

Measured lattice spacing /Å	Calculated lattice spacing /Å	(hkl)
25.5	26.0	(001)
13.0	13.0	(002)
8.68	8.68	(003)
6.51	6.51	(004)
5.21	5.20	(005)
4.34	4.34	(006)
3.72	3.72	(007)
3.41	3.41	(100)

a=3.41 Å, c=26.0 Å.

Table 5. X-Ray Diffraction Data for $Cu(LC_{14})$ at RT

Measured lattice spacing /Å	Calculated lattice spacing /Å	(*hkl*)
24.8	24.9	(001)
12.5	12.4	(002)
9.69	9.69	(010)
8.30	8.30	(003)
6.22	6.22	(004)
4.99	4.98	(005)
4.49	—	—
4.16	4.15	(006)
3.80	—	—
3.56	3.56	(007)
3.45	3.45	(100)

a=3.45 Å, b=9.69 Å, c=24.9 Å.

Table 6. X-Ray Diffraction Data for $Cu(LC_{14})$ at 380 K

Measured lattice spacing /Å	Calculated lattice spacing /Å	(*hkl*)
15.0	15.0	(002)
9.95	10.0	(003)
7.49	7.49	(004)
6.04	5.99	(005)
5.01	5.00	(006)
4.30	4.28	(007)
3.76	3.75	(008)
3.41	3.41	(100)

a=3.41 Å, c=30.0 Å.

Table 7. X-Ray Diffraction Data for $Cu(LC_{16})$ at RT

Measured lattice spacing /Å	Calculated lattice spacing /Å	(*hkl*)
27.4	27.4	(001)
13.7	13.7	(002)
10.1	10.1	(010)
9.15	9.15	(003)
6.84	6.86	(004)
5.46	5.49	(005)
4.53	4.57	(006)
4.48	—	—
3.91	3.92	(007)
3.78	—	—
3.45	3.45	(100)
3.37	3.36	(300)
3.25	3.26	(110)

a=3.45 Å, b=10.1 Å, c=27.4 Å.

$Pd(LC_{16})$ and $Pd(LC'_{16})_2$ do not show a mesophase transition by DSC. $Cu(LC_{16})$ clearly shows a mesophase transition, which is obscure for $Ni(LC_{16})$ and $Co(LC_{16})$. Such a difference in the thermal properties may reflect the character of the central metals. These are probably due to the stacking structure of the core groups.

Other $Cu(LC_n)$ at 380 K also showed spacings assignable to the (00l) spacings, and an intra dimer spacing at 3.39±0.02 Å, indicating that the intra dimer

Table 8. X-Ray Diffraction Data for $Cu(LC_{16})$ at 380 K

Measured lattice spacing /Å	Calculated lattice spacing /Å	(*hkl*)
16.1	16.4	(002)
10.9	10.9	(003)
8.18	8.18	(004)
6.58	6.55	(005)
4.71	4.68	(007)
4.12	4.09	(008)
3.38	3.38	(100)

a=3.38 Å, c=32.8 Å.

Table 9. X-Ray Diffraction Data for $Cu(LC_{18})$ at RT

Measured lattice spacing /Å	Calculated lattice spacing /Å	(*hkl*)
14.9	14.9	(002)
10.7	10.7	(010)
9.97	9.91	(003)
7.47	7.43	(004)
6.05	5.95	(005)
4.97	4.95	(006)
4.53	—	—
4.51	—	—
4.25	4.25	(007)
3.79	—	—
3.73	3.72	(008)
3.44	3.45	(100)
3.27	3.28	(110)

a=3.45 Å, b=10.7 Å, c=29.7 Å.

distances are constant regardless of the methylene number. The c value vs. acyl number (n) plots show a good linearity (Fig. 6), indicating that the alkyl chains are nearly straightened and that the c value increases 3.28 Å with an increase of two methylenes. The sp^3 carbons with a bond length 1.54 Å and a bond angle 109.5° require the interatomic distance to be 2.52 Å, and the dimer conformation requires that to be 5.03 Å for a lengthening of the alkyl chain by two methylene groups. From the observed increase in the c value, 3.28 Å, it is suggested that one of the alkyl chains forms an angle of about 41° to the layer, so as to assign the mesophase of $Cu(LC_n)$ as the smectic C.

At room temperature, the spacings of $Cu(LC_{16})$ at 27.4, 13.7, 9.14, and 6.84 Å are assigned to (001), (002), (003), and (004), planes respectively (c=27.4 Å), to indicate a 5.3 Å decrease in the c value compared to that observed at 380 K. The spacing at 3.45 Å is assigned to the intra dimer distance, indicating that the distance of the two copper atoms increases by 0.07 Å compared to that at 380 K. $Cu(LC_{16})$ also shows a new spacing at 10.1 Å, probably reflecting the orientation of the molecules in the layer (b=10.1 Å).

The c values of $Cu(LC_n)$ at RT showed good linearity for $n \leqq 18$ (Fig. 6) to indicate that the inter-layer distance increases by 2.54 Å for an addition of two methyl-

Table 10. X-Ray Diffraction Data for $Cu(LC_{18})$ at 380 K

Measured lattice spacing /Å	Calculated lattice spacing /Å	(*hkl*)
18.0	18.1	(002)
12.1	12.1	(003)
9.08	9.06	(004)
7.26	7.27	(005)
6.06	6.05	(006)
5.20	5.19	(007)
4.55	4.54	(008)
4.06	4.04	(009)
3.40	3.40	(100)

a=3.40 Å, c=36.2 Å.

Table 11. X-Ray Diffraction Data for $Cu(LC_{20})$ at RT

Measured lattice spacing /Å	Calculated lattice spacing /Å	(*hkl*)
18.4	18.5	(002)
12.3	12.3	(003)
9.24	9.24	(004)
7.38	7.39	(005)
6.15	6.16	(006)
4.80	—	—
4.60	4.62	(008)
4.51	—	—
4.10	4.11	(009)
4.02	—	—
3.40	—	a)
3.30	—	a)

c=37.0 Å. a) Probably reflecting the inter dimer distance.

Table 12. X-Ray Diffraction Data for $Cu(LC_{20})$ at 380 K

Measured lattice spacing /Å	Calculated lattice spacing /Å	(*hkl*)
19.6	19.7	(002)
13.1	13.1	(003)
9.86	9.86	(004)
7.91	7.89	(005)
3.47	—	
3.39	3.39	(100)

a=3.39 Å, c=39.4 Å.

ene groups in $Cu(LC_n)$. It is also suggested that one of the alkyl chains forms an angle 30° to the layer. These complexes also showed spacings at 3.44 or 3.45 Å for the intra dimer distance, which are larger than those in the smectic C phase (Fig. 7). One of the spacings observed at 3.78—4.66 Å probably corresponds to the inter dimer distance. The spacing at 10.1 Å observed in $Cu(LC_{16})$ also increases linearly to the acyl number to indicate the presence of a columnar structure in the layer of which the distance is increased by 0.53 Å for an addition of two methylene groups.

On the other hand, $Cu(LC_{20})$ showed an inter-layer distance at 37.0 Å. The results of DSC suggest that

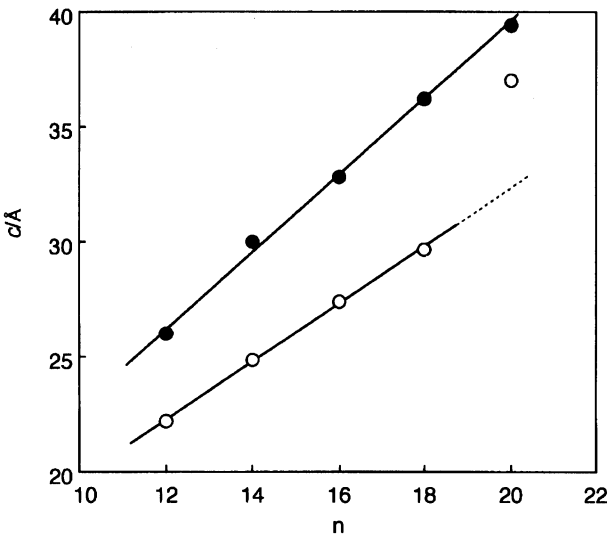

Fig. 6. Observed c values of $Cu(LC_n)$ as a function of n. ●: at 380 K; ○: at RT.

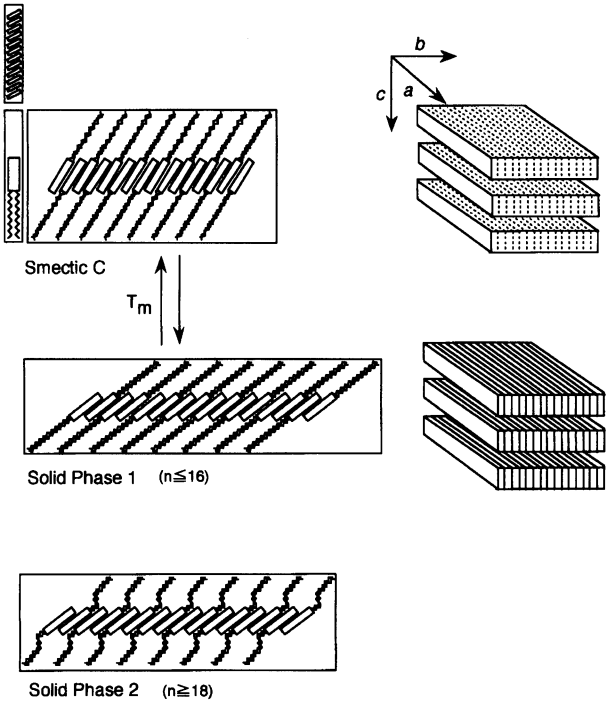

Fig. 7. Proposed stacking model for $Cu(LC_n)$.

the alkyl chains of $Cu(LC_{20})$ which exist folded at RT restacked to form an extended straight conformation during the heating process, showing characteristic endo- and exothermic peaks at T_{t1}, T_{t2}, and T_{t3} in DSC.

References

1) S. Kugiyama and M. Takemura, *Tetrahedron Lett.*, **31**, 3157 (1990).

2) Y. Shimizu, M. Miya, A. Nagata, K. Ohta, A. Matsumura, I. Yamamoto, and S. Kusabayashi, *Chem. Lett.*, **1991**, 25.

3) Z. Belarbi, C. Sirlin, J. Simon, and J. -J. Andre, *J. Am. Chem. Soc.*, **93**, 8105 (1989).

4) K. Ohta, Y. Morizumi, H. Akimoto, O. Takenaka, T. Fujimoto, and I. Yamamoto, *Mol. Cryst. Liq. Cryst.*, **214**, 143 (1992); K. Ohta, Y. Morizumi, H. Ema, T. Fujimoto, and I. Yamamoto, *Mol. Cryst. Liq. Cryst.*, **208**, 55 (1991); K. Ohta, T. Watanabe, H. Hasebe, Y. Morizumi, T. Fujimoto, and I. Yamamoto, *Mol. Cryst. Liq. Cryst.*, **196**, 13 (1991).

5) K. Ohta, O. Takenaka, H. Hasebe, Y. Morizumi, T. Fujimoto, and I. Yamamoto, *Mol. Cryst. Liq. Cryst.*, **195**, 135 (1991).

6) N. Kishii, K. Araki, and S. Shiraishi, *Bull. Chem. Soc. Jpn.*, **57**, 2121 (1984).

7) M. Yamada, K. Araki, and S. Shiraishi, *Bull. Chem. Soc. Jpn.*, **60**, 3149 (1987).

8) E. N. Baker, D. Hall, and T. N. Waters, *J. Chem. Soc. A*, **1970**, 406.